CONFIDENTIAL

~~UNAVAILABLE~~
Copy 1
RM SL55J11

~~UNAVAILABLE~~

NACA

RESEARCH MEMORANDUM

for the

U. S. Air Force

QUALITATIVE RESULTS FROM A FLIGHT INVESTIGATION TO

DETERMINE AILERON EFFECTIVENESS OF TWO

ROCKET-PROPELLED 1/20-SCALE MODELS OF

THE MX-776 MISSILE

By Joseph E. Stevens

Langley Aeronautical Laboratory
Langley Field, Va.

NATIONAL ADVISORY COMMITTEE
FOR AERONAUTICS

WASHINGTON

OCT 20 1955

15

CONFIDENTIAL

NATIONAL ADVISORY COMMITTEE FOR AERONAUTICS

RESEARCH MEMORANDUM

for the

U. S. Air Force

QUALITATIVE RESULTS FROM A FLIGHT INVESTIGATION TO DETERMINE AILERON EFFECTIVENESS OF TWO ROCKET-PROPELLED 1/20-SCALE MODELS OF THE MX-776 MISSILE

By Joseph E. Stevens

SUMMARY

Free-flight tests of two rocket-propelled 1/20-scale models of the Bell MX-776 missile have been conducted to obtain measurements of the aileron deflection required to counteract the induced rolling moments caused by combined angles of attack and sideslip and thus to determine whether the ailerons provided were capable of controlling the model at the attitudes produced by the test conditions. Inability to obtain reasonably steady-state conditions and superimposed high-frequency oscillations in the data precluded any detailed analysis of the results obtained from the tests. For these reasons, the data presented are limited largely to qualitative results.

INTRODUCTION

The Pilotless Aircraft Research Division, at the request of the Air Materiel Command, U. S. Air Force, has conducted tests of two 1/20-scale rocket-propelled models of the Bell MX-776. The purpose of these tests was to obtain a measure of the aileron deflection required to counteract the induced rolling moments caused by combined angles of attack and sideslip in an effort to determine whether the ailerons provided were capable of controlling the model at the attitudes produced by the test conditions.

The apparatus employed to obtain the test conditions was a relatively complex static type of mechanism propelled to low supersonic

speeds by a rocket motor. Dynamic responses of the mechanism, not anticipated in the basic engineering design, practically obscured the static response desired. For this reason, no detailed analysis is possible and data presented are limited largely to qualitative results.

SYMBOLS

δ_T total differential deflection of two ailerons, deg

M Mach number

C_h hinge-moment coefficient of two ailerons, $\frac{H}{qS_a c_a}$

H total hinge moment of two ailerons, in-lb

q dynamic pressure, lb/sq ft

S_a area of two ailerons behind the hinge line, sq ft

c_a mean aileron chord, ft

α angle of attack of test vehicle, deg

α_s angle of attack of sting and model, deg

β angle of sideslip of the test vehicle, deg

ϕ roll angle of model with respect to sting (zero when model vertical plane of symmetry coincided with sting vertical plane of symmetry and model cutout fin was down as in fig. 2), deg

MODELS AND INSTRUMENTATION

Geometric details of the models tested are presented in figure 1 and table I. Figure 1 actually shows model B with its deflected canard control surfaces whereas the controls on model A were undeflected. The 1/20-scale model was mounted on a sting which was attached at a fixed angle of incidence to the forward end of a rocket test vehicle as shown in figures 2 and 3. The model was free to roll about the inclined sting axis. The test vehicle was composed of an ABL Deacon rocket motor with stabilizing fins, the model, and a section between the model and rocket

to house the aileron driving mechanism and telemetering instrumentation. Small, fixed, deflected trimmer fins on the forward end of the vehicle were used to approximately counteract the pitching moment caused by the sting-mounted model and thus keep the test vehicle at small angles of attack during the test flight.

The model fuselage was machined from solid aluminum alloy and the wings and fins were machined from steel and pinned to the fuselage. Twenty-five-percent-chord, approximately full-span ailerons were hinged to the rear horizontal surfaces and served to roll the model during the major portion of the tests. The two models, model A and model B, were identical with one exception: the forward surfaces of model A were not deflected; while on model B the 25-percent-chord elevator on the forward horizontal fin was deflected 30° with the trailing edge up and the all-movable forward vertical fin was deflected 30° with the trailing edge to the right. These deflections were such as to trim the model for positive side force and negative lift.

Figure 4 shows some of the internal instrumentation and mechanism used to produce the test conditions. Through an inner shaft and bevel gears an electric motor mechanically deflected the ailerons continuously in one direction which in turn drove the free rolling model aerodynamically.

Aileron deflection was determined by the angular relationship between the inner drive shaft and the outer support shaft which was an integral part of the model. The roll position of the model with respect to the sting was ascertained from a cam mounted on the model support shaft. Hinge moments were measured as secondary data at the bearing-mounted motor through a restricting beam. Transverse and normal accelerometers were mounted in the rear portion of the telemeter section (fig. 3) near the center of gravity of the complete configuration. Angle-of-attack and angle-of-sideslip indicators were affixed to the tips of the bottom vertical and right horizontal stabilizing fins, respectively. Additional test information was obtained using a CW Doppler velocimeter radar set, a modified SCR-584 radar tracking set and radiosondes released immediately after the test flights. Motion pictures also were taken of the early portions of the flights.

TEST TECHNIQUE

The purpose of the tests reported herein was to obtain a measure of the aileron deflection required to counteract the induced rolling moments caused by combined angles of attack and sideslip. The combined angles were produced by roll angles occurring on the model with its longitudinal axis inclined at a fixed angle with respect to the vehicle flight path.

The model ailerons were deflected continuously in one direction by an electric drive motor and gearing arrangement. As the model rolled in response to the aileron aerodynamic rolling moment, the gearing operated to reduce the aileron deflection and the freely-rolling model tended to seek a roll rate such that it was in equilibrium with regard to rolling moments.

The original concept of the technique employed in these tests assumed that relatively steady-state conditions would exist during the flight tests and direct results could be obtained from the data. Several factors made this assumption invalid. Torsional vibrations in the mechanism practically obscured the basic data and rapid deceleration through the speed range allowed too little time for the steady-state conditions to be attained. In addition, friction loads due to longitudinal acceleration distorted some of the data.

The primary objective of the current tests was to obtain cross plots of δ_T against φ from which approximate values of aerodynamic rolling derivatives could be obtained, and an analysis of the data was attempted using a curve-fitting procedure to extract the basic data desired; but no satisfactory results could be obtained. It is felt that a much more complex mechanical system would be required to obtain satisfactory results from the technique.

PRESENTATION OF RESULTS

Time histories of the data obtained from the decelerating portions of the two test flights are presented in figures 5 and 6. The quantities illustrated are Mach number, total differential deflection of two ailerons, total hinge-moment coefficient of two ailerons, roll angle of the model with respect to the test vehicle, and angle of attack and angle of sideslip of the complete test vehicle.

Data obtained from model A are presented in figure 5(a) for roll cycles in the Mach number range between 1.31 and 0.64 and in figure 5(b) for one roll cycle at an average Mach number of about 0.49. Near the maximum velocity of the test flight both the angle-of-attack and angle-of-sideslip indicator vanes began to buzz. After about 1.5 seconds the buzz disappeared but the sideslip vane had apparently suffered physical damage and remained against the 15° limit stop for the remainder of the flight. Sideslip information shown in figure 5 was computed using data from the transverse accelerometer and an estimated variation of side force with angle of sideslip.

When first plotted, the values of aileron deflection for model A indicated predominantly positive values with only occasional small

negative values being attained. A considerable amount of time spent in trying to analyze the data led to the conclusion that an error probably existed in ascertaining the zero value of aileron deflection from the flight record. Examination of crossplots of δ_T against φ and C_h against δ_T indicated that this error was about -10°. All of the aileron deflection values shown in figure 5 have had this correction applied. Thus, while the absolute magnitudes of all the values of δ_T are questionable, the variations with time or roll angle should be reliable.

During the first complete roll cycle during coasting flight, the Mach number and angle of attack are changing rapidly and the aileron deflection does not indicate a repetitive character. Subsequent roll cycles indicate a more nearly repetitive aileron-deflection record with a basic frequency four times the roll frequency. The hinge-moment coefficient data exhibit the same basic frequency and also show a persistent high-frequency oscillation which in the Mach number range from 1.1 to 0.8 becomes so severe that it almost obscures the basic wave form. This high-frequency oscillation also occurs in the aileron-deflection data but to a much smaller extent and does not appear to have affected the roll-angle data. The cause of this high-frequency oscillation is not certain but two possible sources have been considered. Because it appears primarily in the hinge-moment data and at transonic speeds it may be an indication that the inboard ends of the ailerons are being buffeted by separated air flow from the rather blunt afterbody of the model (see top view, fig. 1). This effect is probably aggravated by any compression wave formed by the cone-shaped sting immediately to the rear of the model. A second or additional source of the oscillation may be a torsional vibration in the model-rolling mechanism.

Figure 6 presents the time history of the data obtained from model B. As stated previously, the forward control surfaces on model B were deflected whereas those on model A were not. Data for model B were obtained over the Mach number range between 1.32 and 0.67. Oscillations of about 15 cycles per second practically obscure the basic wave form of δ_T and C_h for this model also, and are even more severe than the similar oscillations occurring in the data from model A.

Figures 7 (for model A) and 8 (for model B) show plots of Mach number, total aileron deflection, and sting angle of attack (angle of attack of test vehicle plus sting skew angle of 15°) against roll angle of the model for each of the complete roll cycles illustrated in figures 5 and 6, respectively.

The data for model A in figures 7(a), (b), (c), and (d) generally exhibit the expected variation with δ_T, having four times the roll

frequency as mentioned previously with zero values near the positions of symmetry ($\varphi = 0^{\circ}$, 90°, 180°, and 270°). Less obvious but also present in the data is a still lower frequency of twice the roll frequency. Physical considerations based on the type of geometrical symmetry of the model confirm that such a frequency should be present due to the differences between the horizontal and vertical surfaces. Examination of the δ_T curves in figure 7 indicates that the values of δ_T are generally larger for angles of roll on either side of the 90° and 270° positions of symmetry than for corresponding angles near the 0° and 180° positions. This indicates that sideslipping the model at small angles of attack generally produces more induced rolling moments than pitching the model at small angles of sideslip. The maximum total aileron deflection required to trim out all rolling moments caused by the angles of attack obtained in the test of model A appears to be about $\pm 10^{\circ}$ at subsonic speeds rising to the order of $\pm 20^{\circ}$ to $\pm 30^{\circ}$ at transonic speeds. Roll damping moments involved in this test are considered negligible since average rates of roll obtained from figure 5 and damping-in-roll data from reference 1 indicate that the total aileron deflection required to counteract the roll damping is about 0.3° at $M = 0.5$ and less at higher Mach numbers.

The data of model B in figures 8(a), (b), (c), and (d) exhibit similar characteristics to the data of model A, with δ_T having a discernible frequency four times the roll rate. More noticeable for this model, however, is the δ_T frequency of twice the roll rate. This difference in the data obtained from the two models is attributed to the deflected canard control surfaces on model B since the required aileron deflections reach maximum values at the roll positions when the angle of attack reaches negative values combined with large positive or negative angles of sideslip. As can be seen by comparing the plots of figure 8, the aileron deflection reaches a maximum negative value when φ is about 120° and a maximum positive value when φ is about 240°, but accurate deflection values are obscured by the superimposed high-frequency oscillations and the fact that the ailerons usually went against their limit stops at the roll angles mentioned above.

CONCLUDING REMARKS

Two free-flight tests of rocket-propelled, 1/20-scale models of the Bell MX-776 missile have been conducted to determine whether the ailerons provided were capable of controlling the models under set conditions of angles of attack combined with angles of sideslip. The results obtained are practically obscured by high-frequency oscillations in the basic data and the inability to obtain reasonably steady-state conditions. The data in general indicate, as would be expected,

that minimum aileron deflections are needed to counteract induced rolling moments caused by combined angles of attack and sideslip when either of the two angles is near zero. With the forward control surfaces deflected to produce positive side force and negative lift, the aileron deflections required are maximum at negative angles of attack combined with positive or negative angles of sideslip. Successful use of the technique employed in these tests would require an extensive analysis of the difficulties encountered and redesign of the mechanisms and apparatus used.

Langley Aeronautical Laboratory,
National Advisory Committee for Aeronautics,
Langley Field, Va., October 3, 1955.

Joseph E. Stevens
Joseph E. Stevens
Aeronautical Research Scientist

Approved: Joseph A. Shortal
Joseph A. Shortal
Chief of Pilotless Aircraft Research Division

BS

REFERENCE

1. Bland, William M., Jr., and Purser, Paul E.: Rocket-Model Measurements of Zero-Lift Damping in Roll of the Bell MX-776 Missile at Mach Numbers from 0.6 to 1.56. NACA RM SL54A13, 1954.

[redacted]

TABLE I

GEOMETRY OF MODELS

Fuselage: Frontal area, 4.53 sq in.; maximum diameter, 2.40 in.; fineness ratio, 8.00

Wing and Fins:

	Rear horizontal wing	Front horizontal wing	Rear vertical fin	Front vertical fin
Total included area, sq in.	32.95	14.65	17.62	4.28
Aspect ratio	3.05	3.22	3.20	3.70
Taper ratio	0.28	0.25	0.26	0.19
Angle of incidence, deg	0	0	0	0
Dihedral, deg	0	0	0	0
Sweep of 0.75 chord, deg	0	0	0	0
Airfoil section (streamwise) . .	Circular arc with full slab back of 0.75 chord	Circular arc with half slab back of 0.75 chord	Circular arc	Double wedge

[redacted]

[redacted]

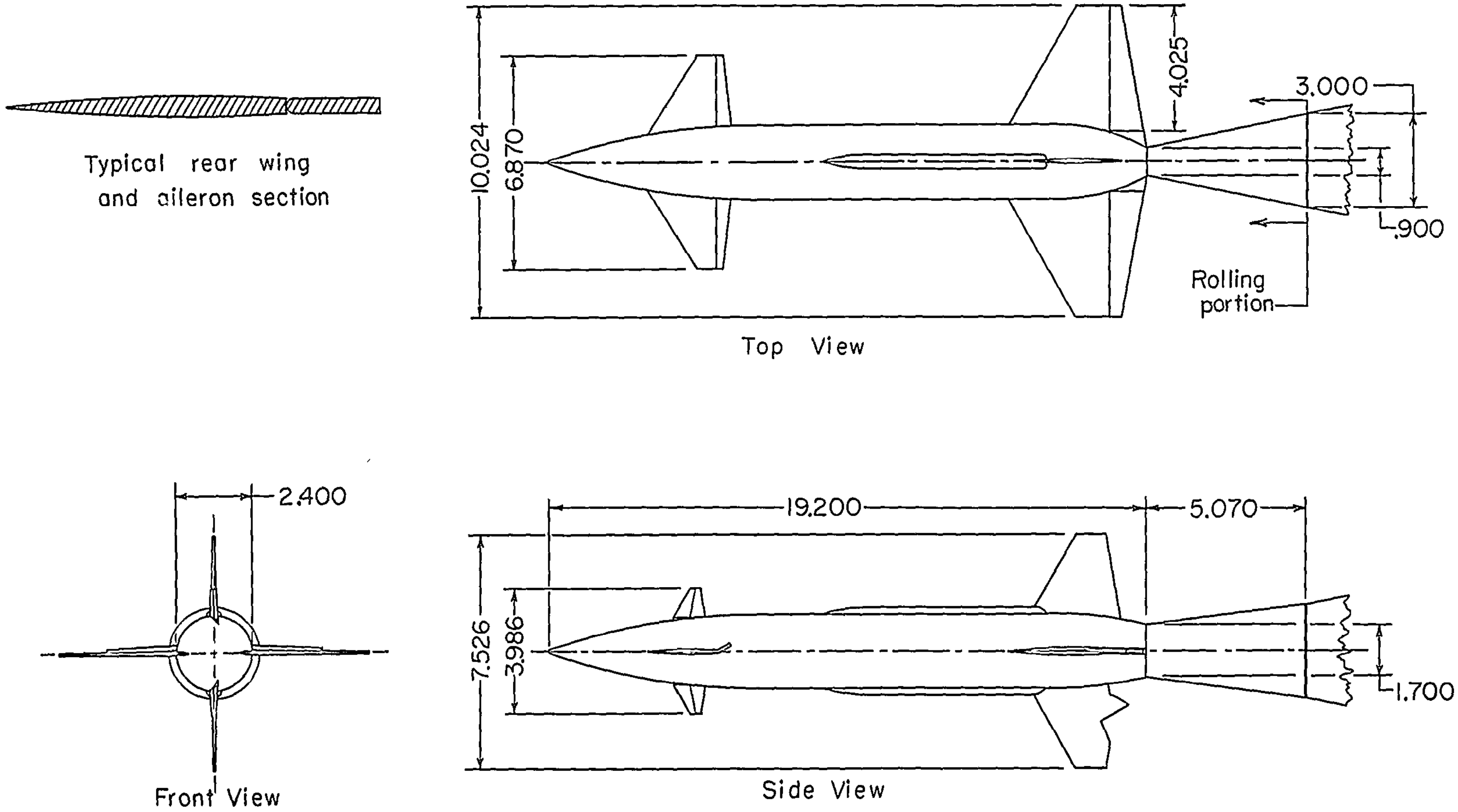

Figure 1.- Three-view drawing of 1/20-scale model. (All dimensions are in inches.)

[redacted]

[redacted]

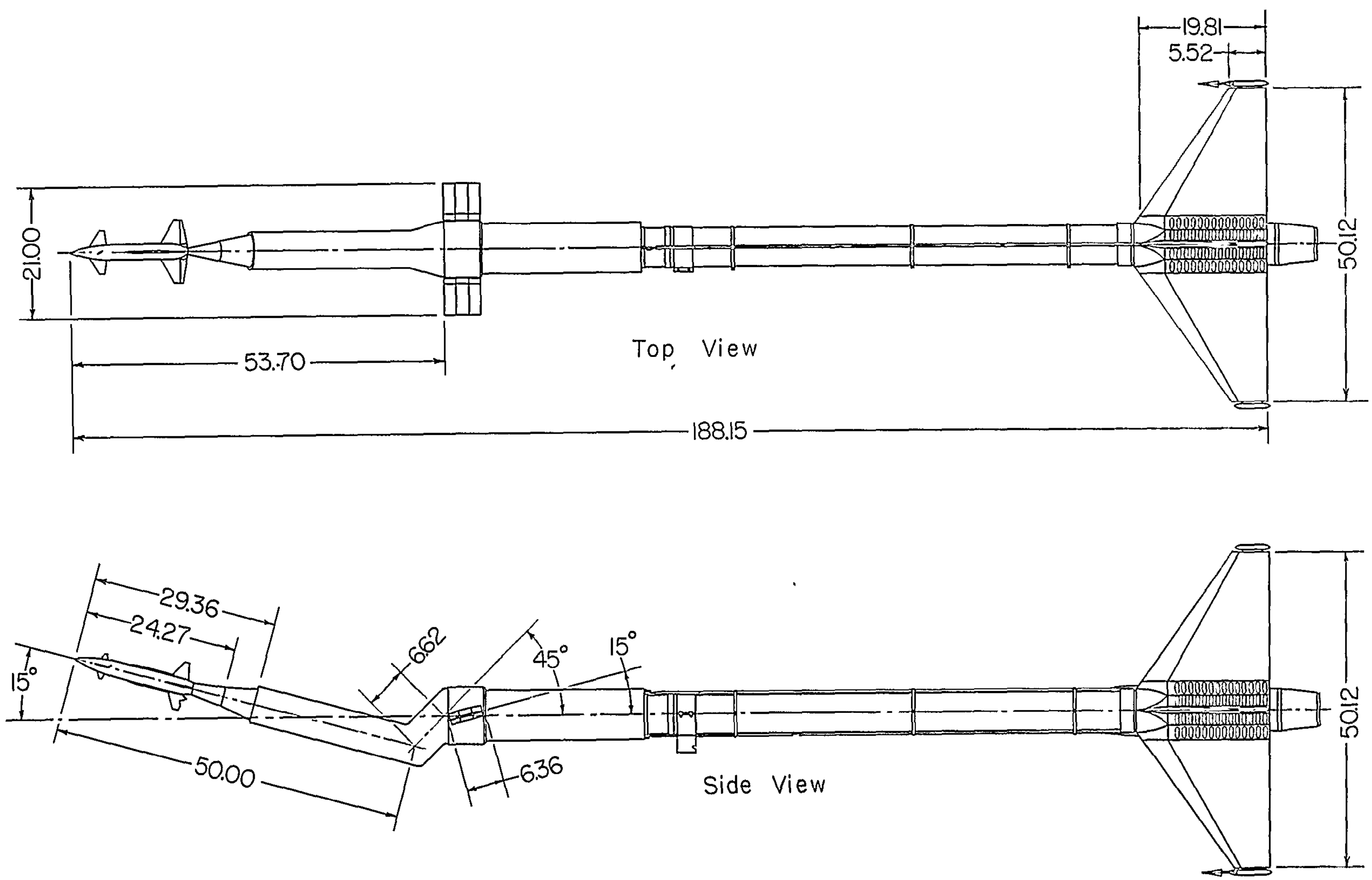

Figure 2.- General arrangement of model and test vehicle. (All dimensions are in inches.)

[redacted]

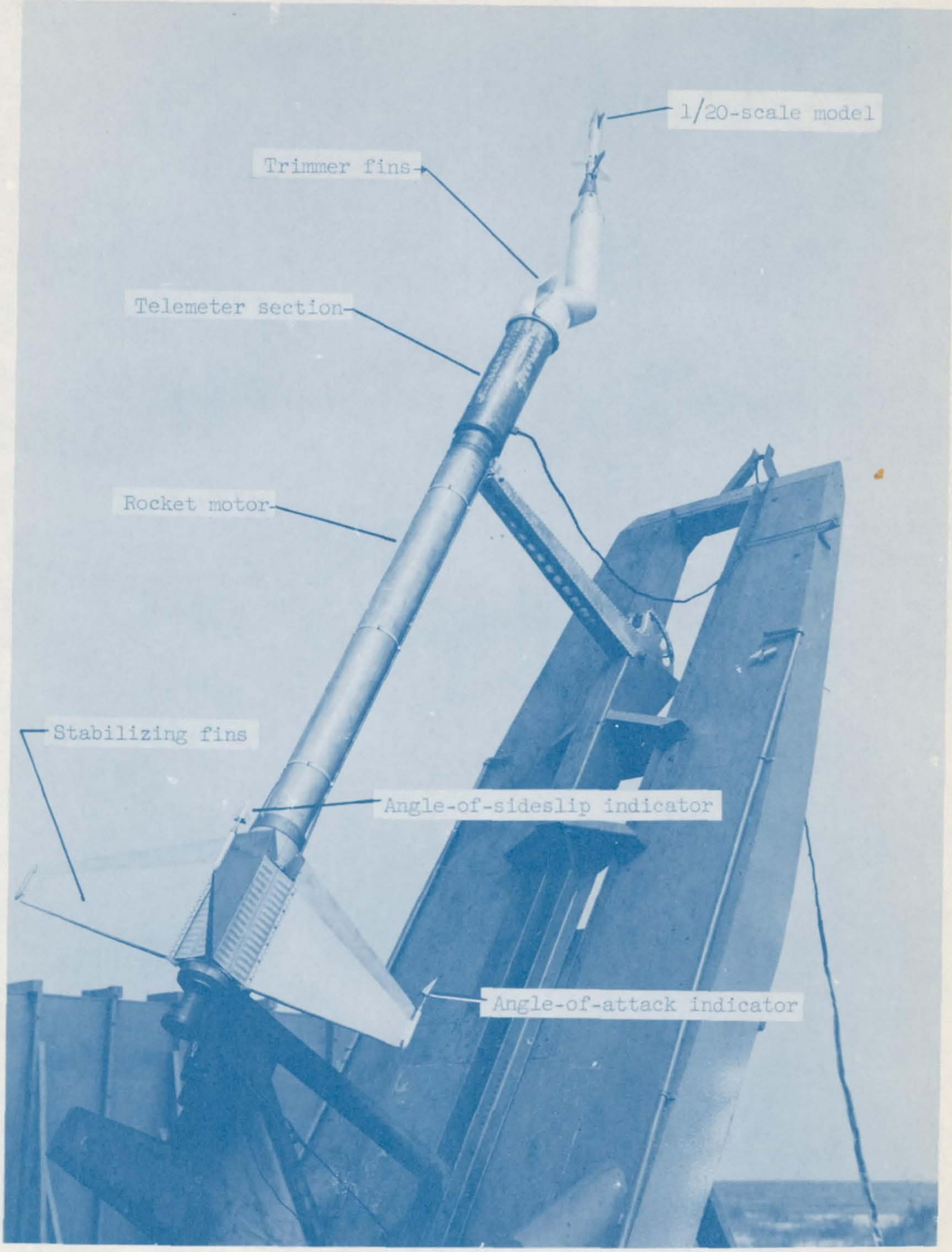

Figure 3.- Complete configuration mounted on launcher. L-81343.1

CONFIDENTIAL

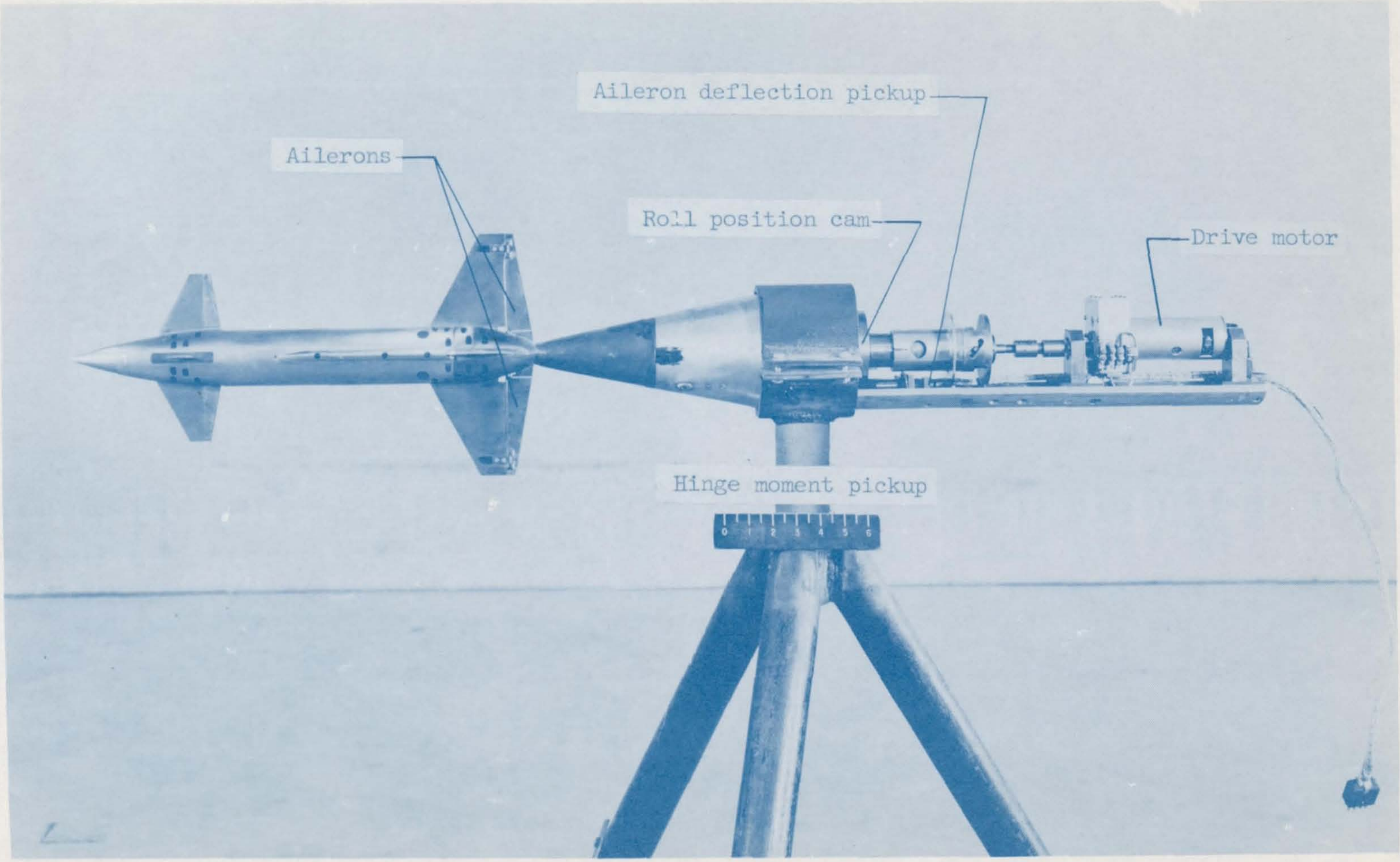

L-81121.1

Figure 4.- Model and sting section showing some of the internal instrumentation.

CONFIDENTIAL

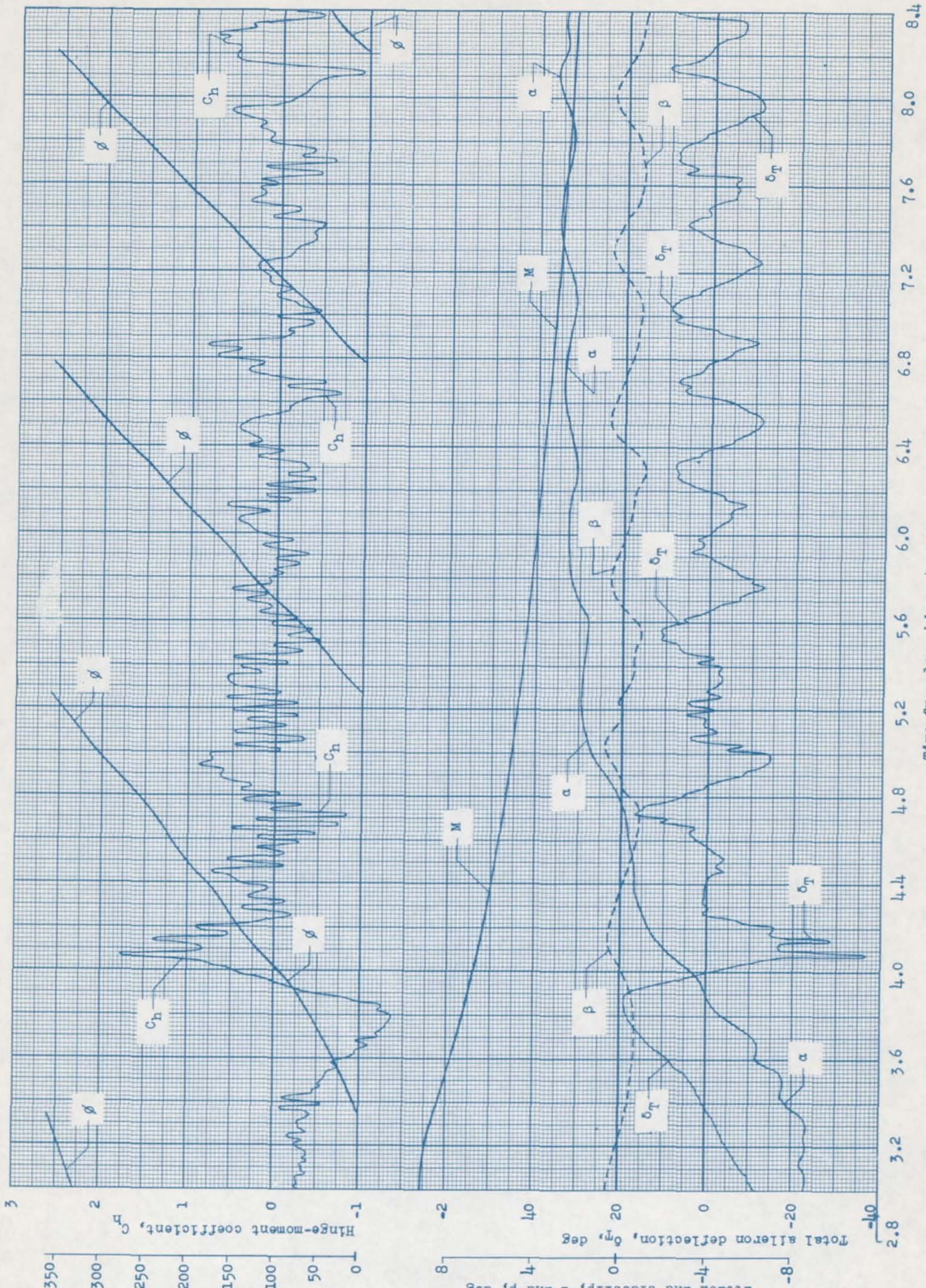

(a) 3.0 to 8.4 seconds.

Figure 5.- Time history obtained from model A.

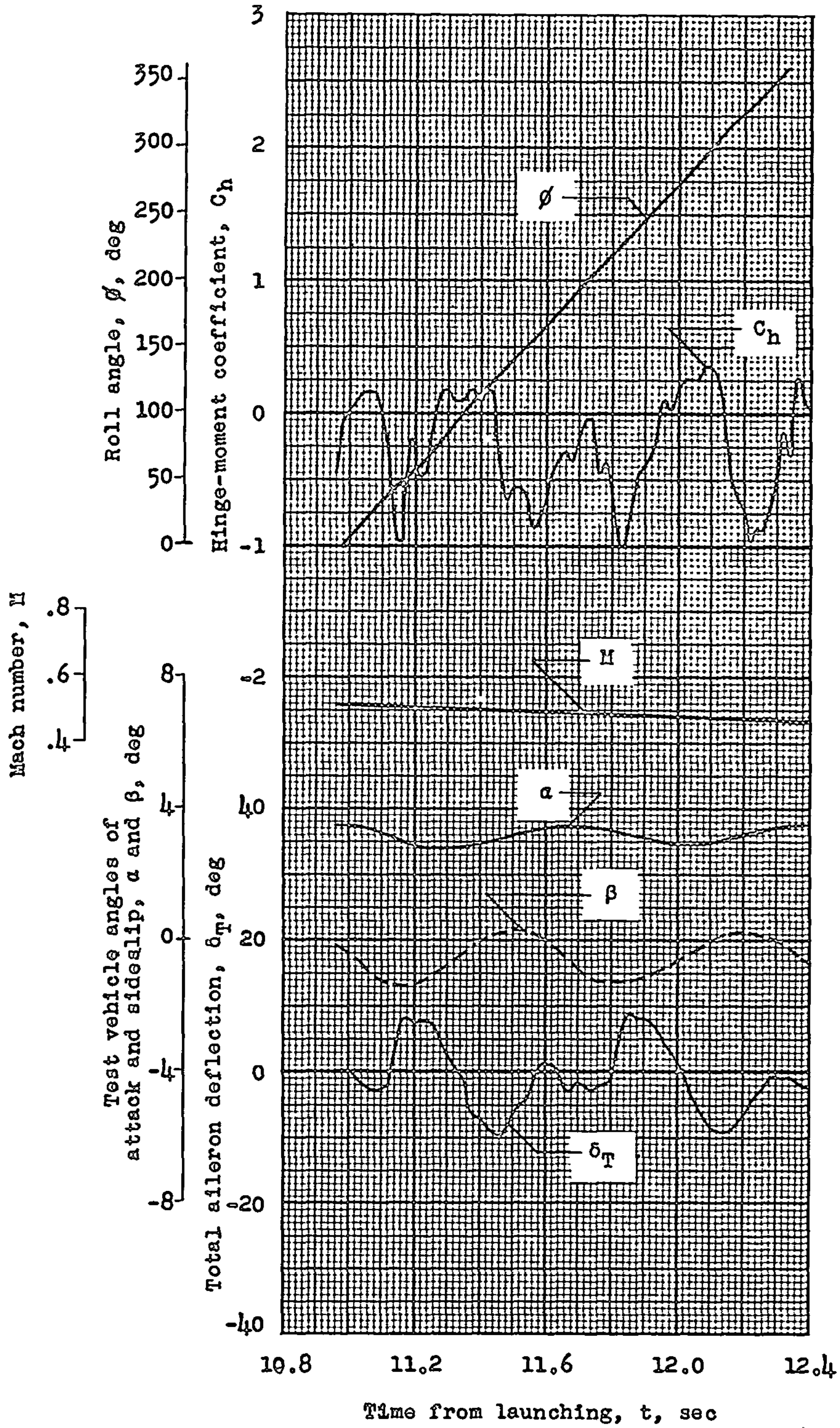

(b) 10.8 to 12.4 seconds.

Figure 5.- Concluded.

[redacted]

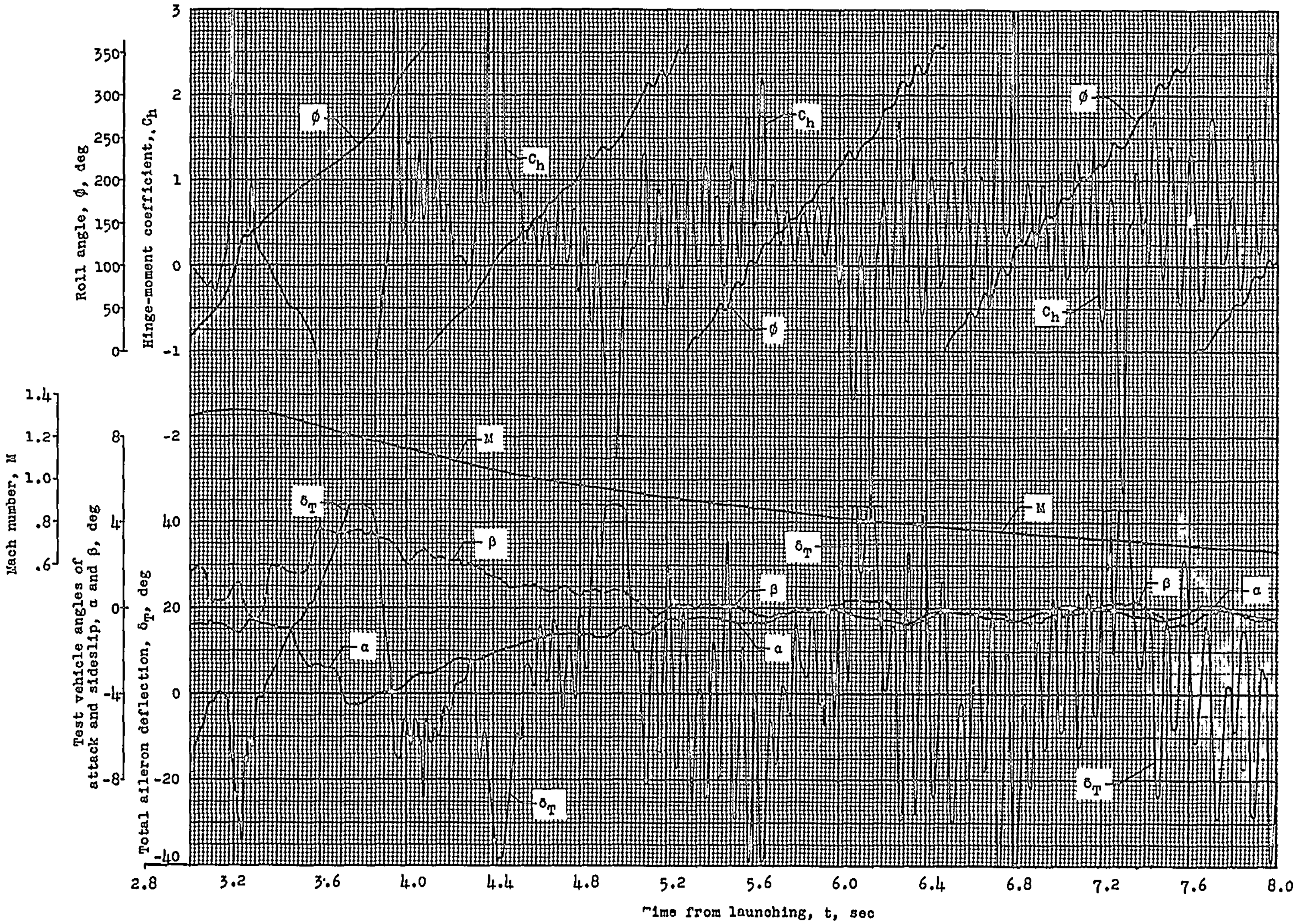

Figure 6.- Time history obtained from model B.

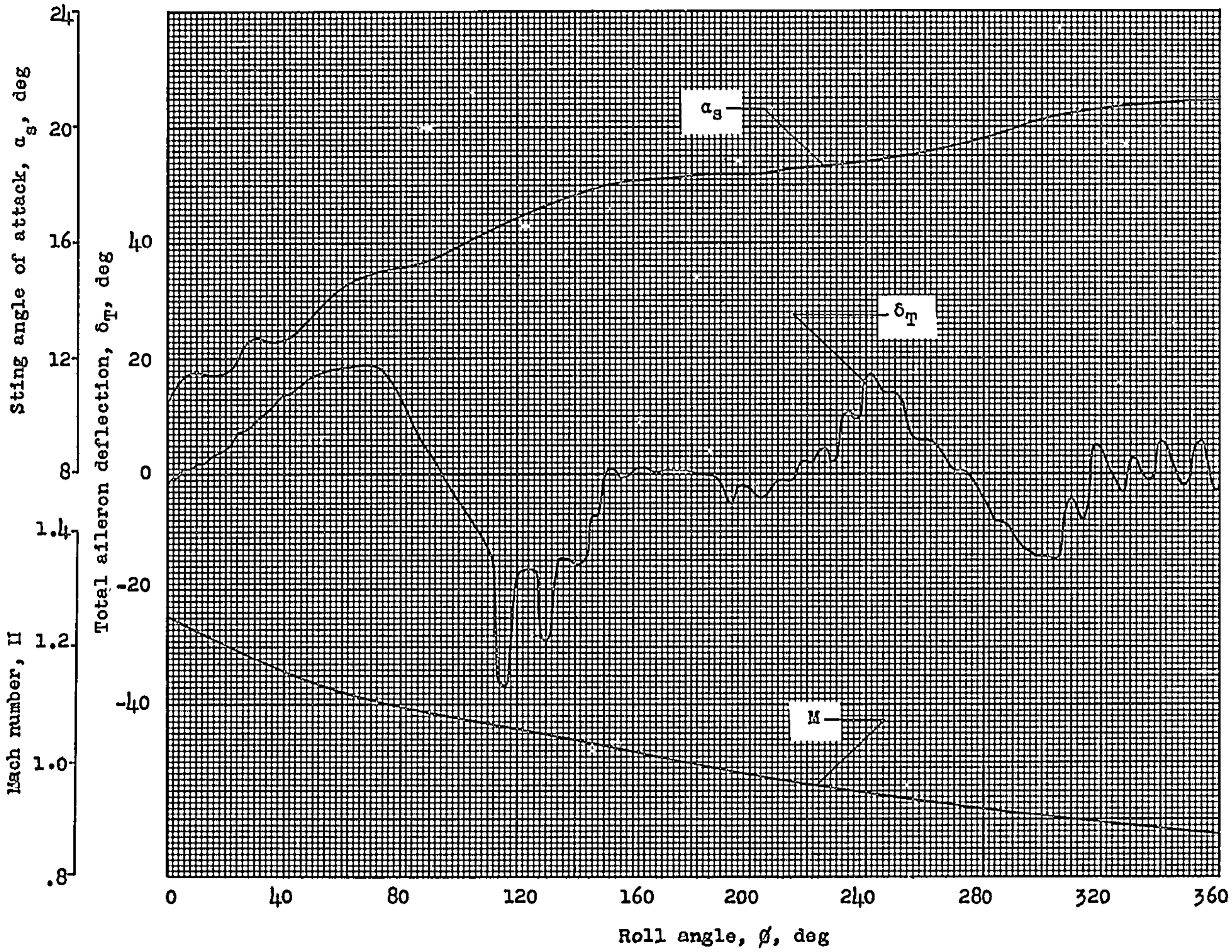

(a) 3.34 to 5.26 seconds.

Figure 7.- Mach number, total aileron deflection, and sting angle of attack as functions of roll angle for model A.

[redacted]

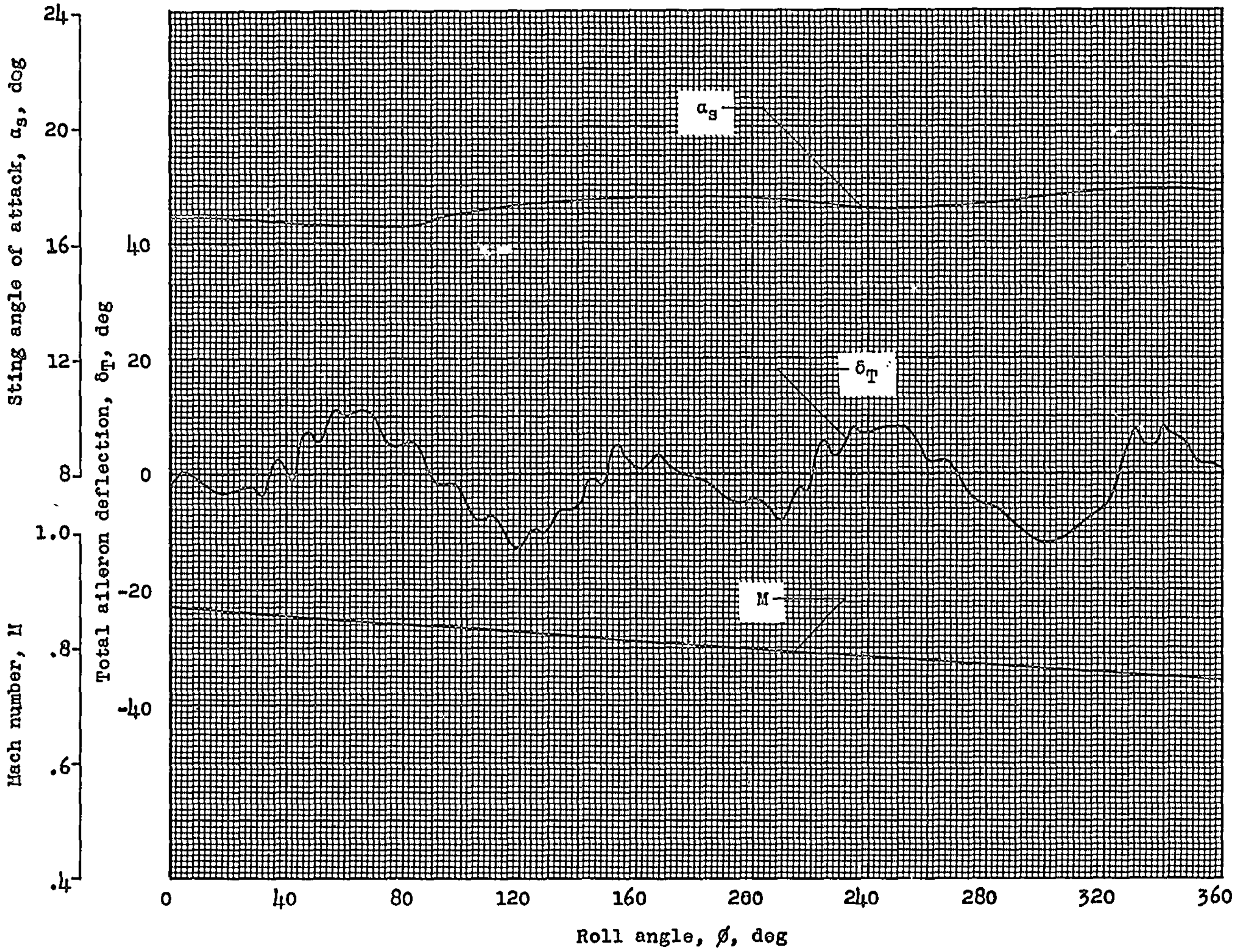

(b) 5.28 to 6.76 seconds.

Figure 7.- Continued.

[redacted]

[redacted]

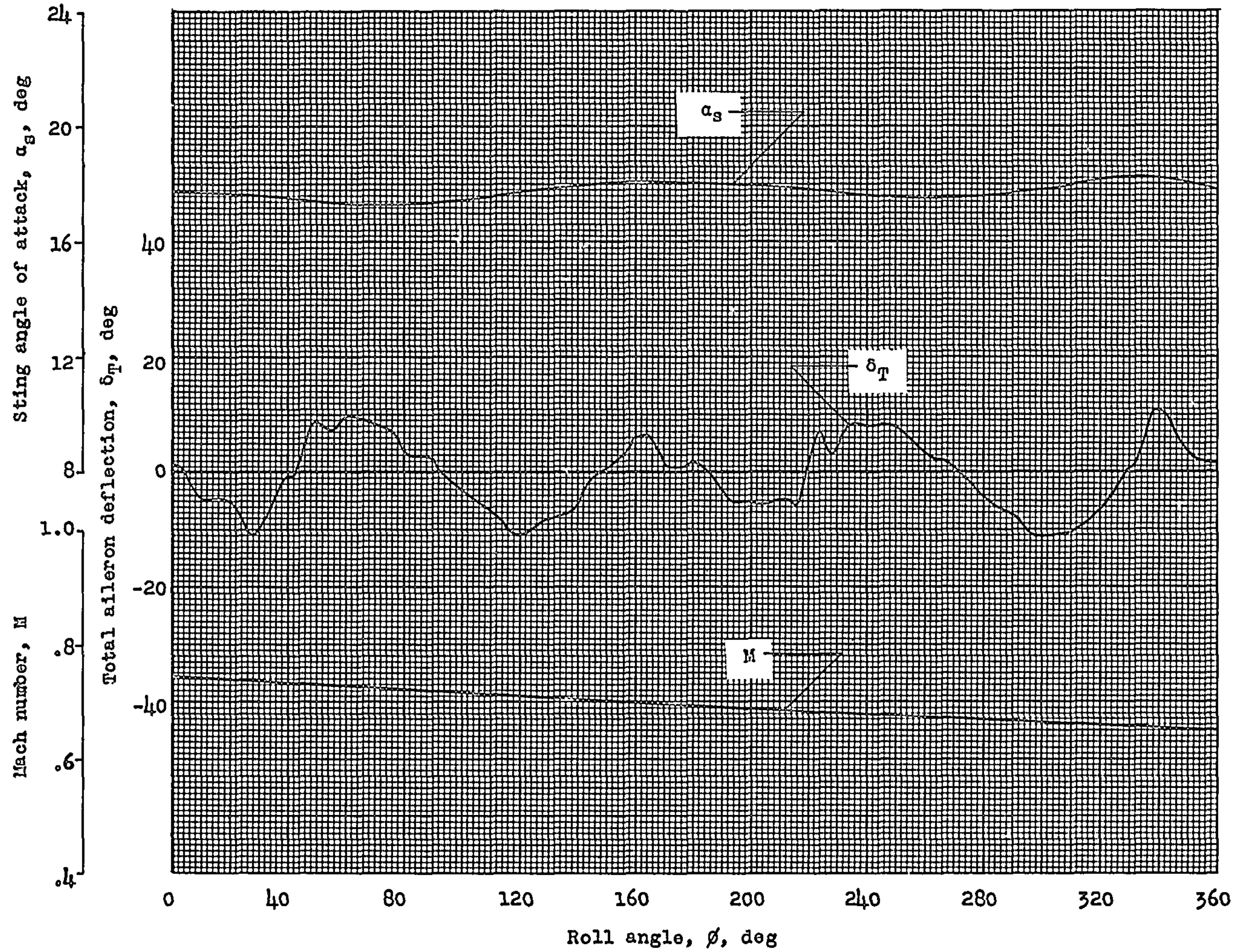

(c) 6.78 to 8.20 seconds.

Figure 7.- Continued.

[redacted]

[redacted]

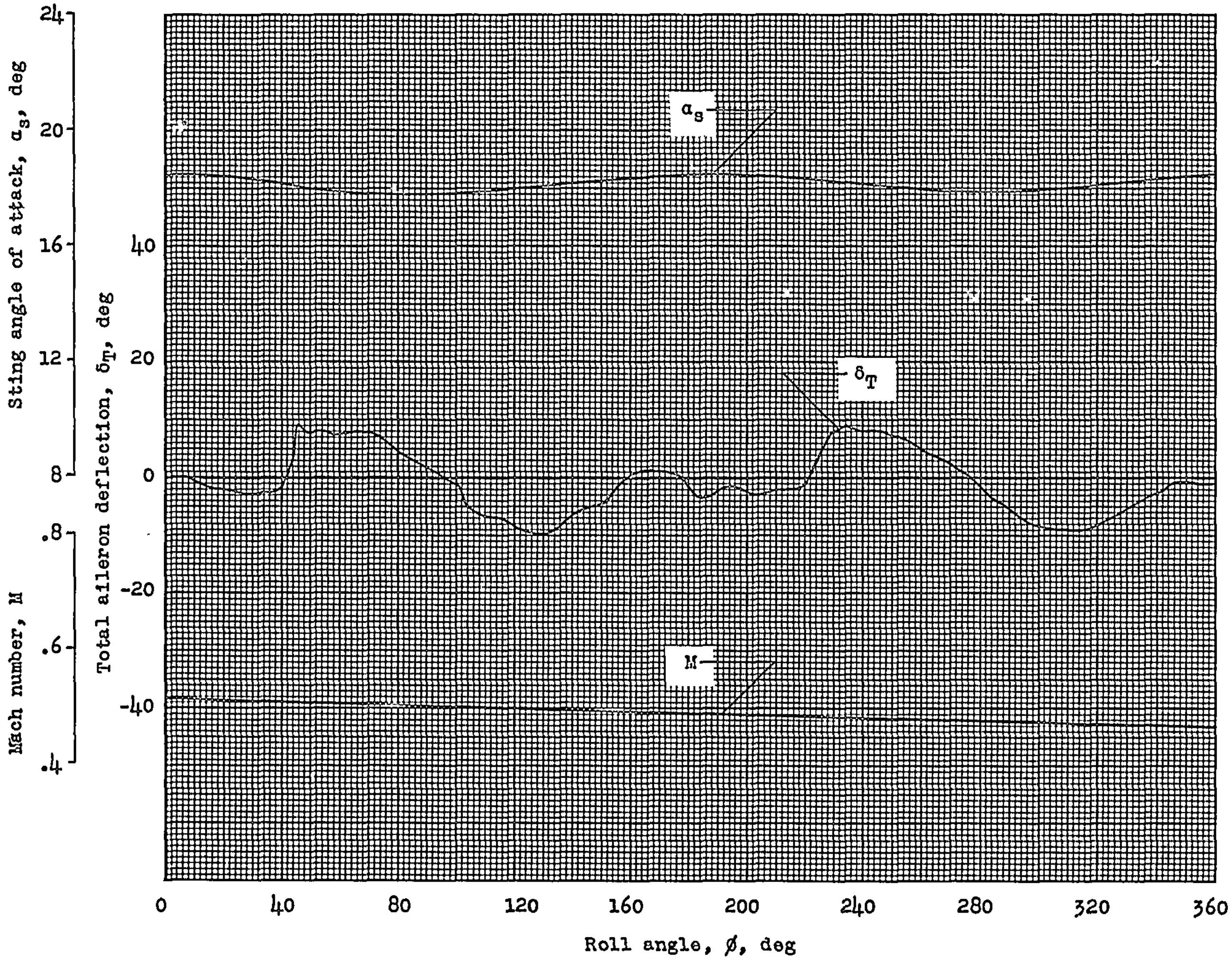

(d) 10.98 to 12.34 seconds.

Figure 7.- Concluded.

[redacted]

[redacted]

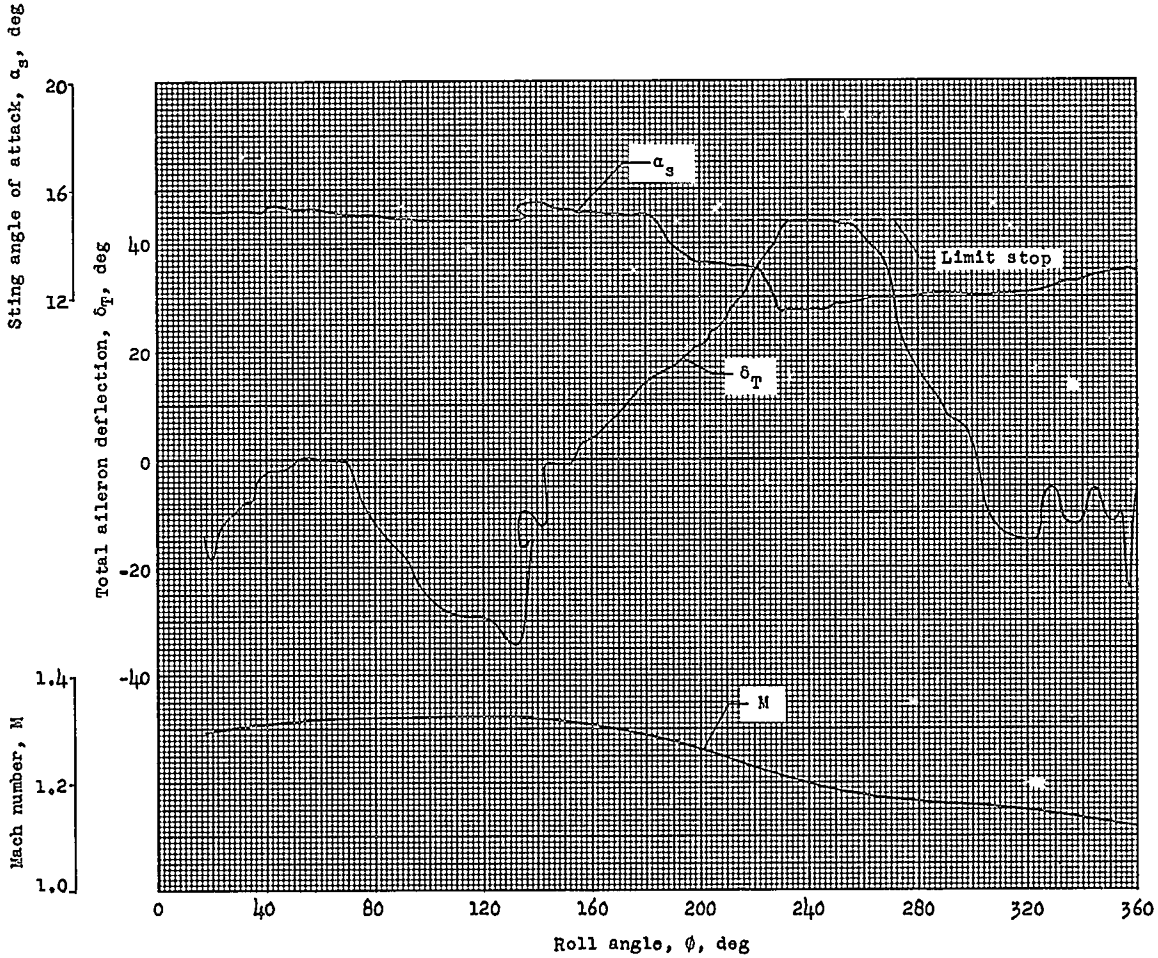

(a) 3.00 to 4.09 seconds.

Figure 8.- Mach number, total aileron deflection, and sting angle of attack as functions of roll angle for model B.

[redacted]

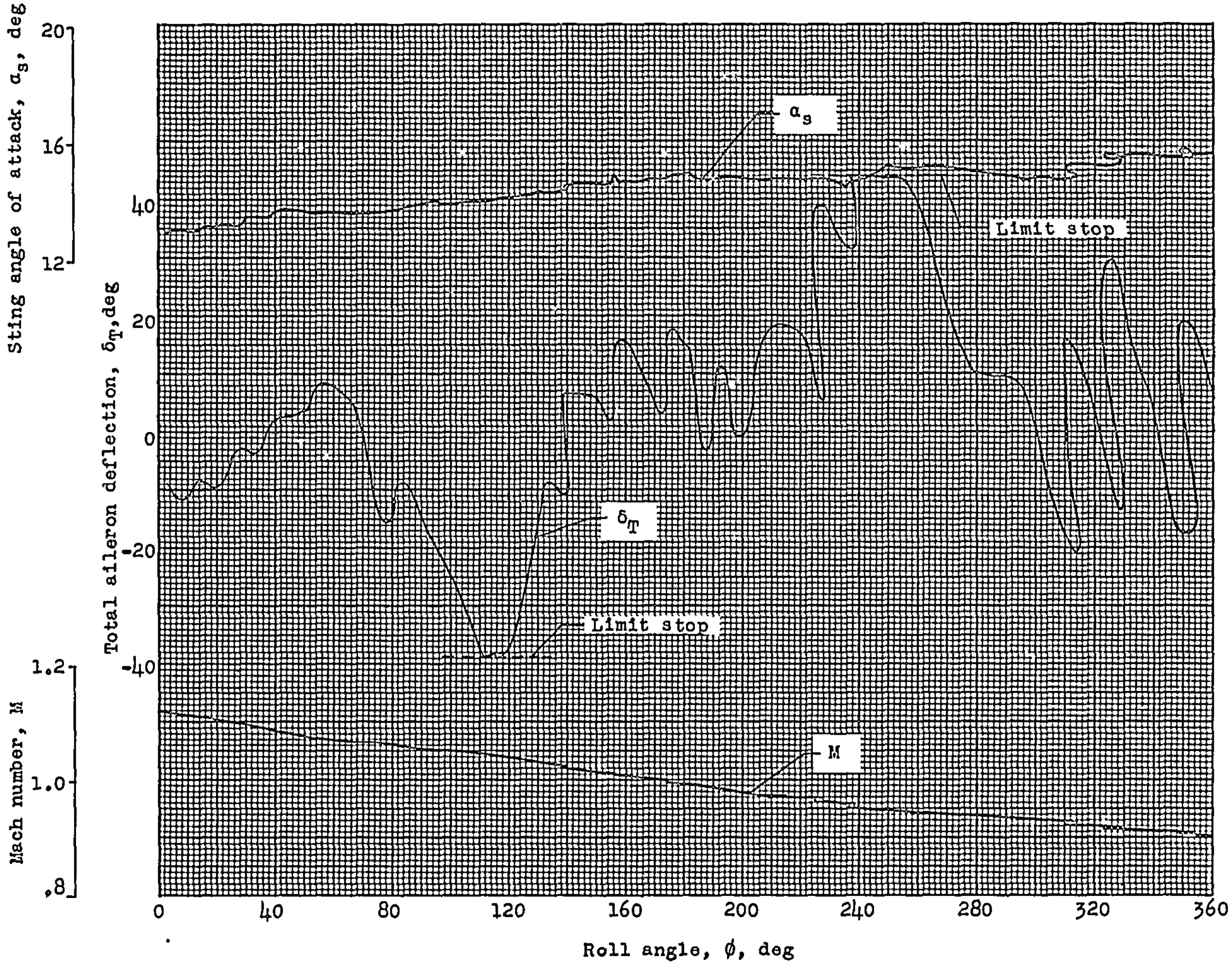

(b) 4.10 to 5.29 seconds.

Figure 8.- Continued.

[redacted]

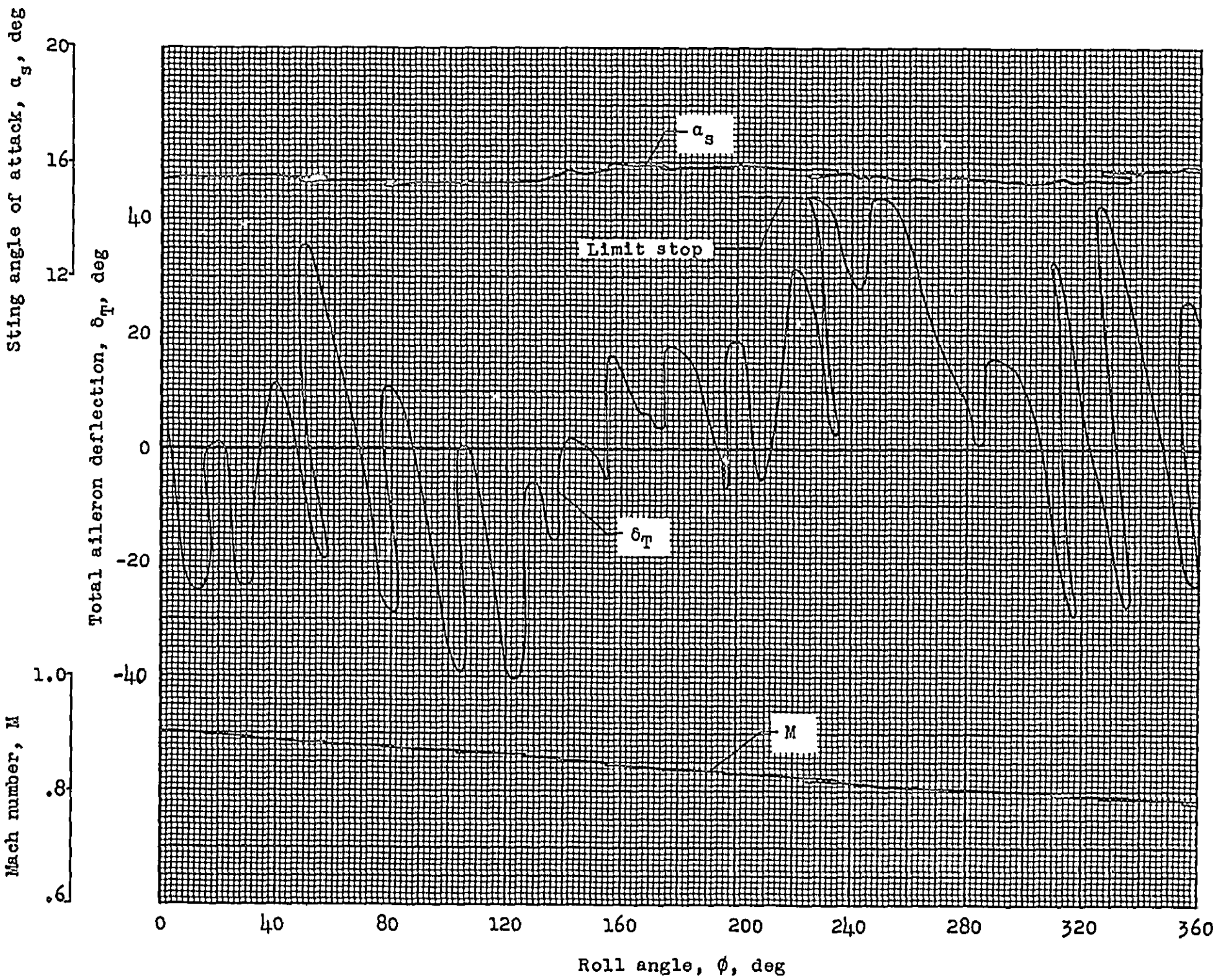

(c) 5.30 to 6.48 seconds.

Figure 8.- Continued.

[redacted]

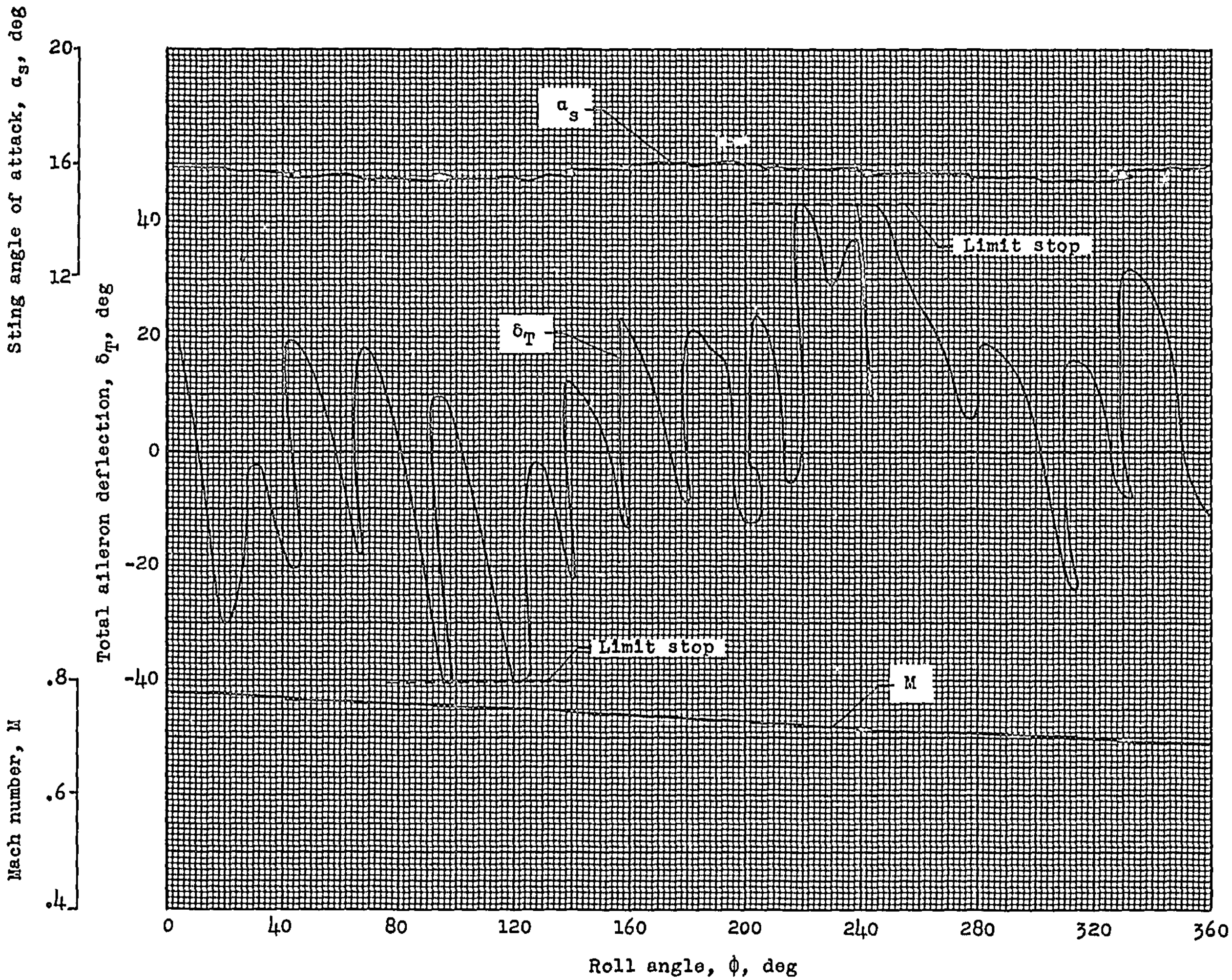

(d) 6.49 to 7.62 seconds.

Figure 8.- Concluded.